Journal of Electroanalytical Chemistry 645 (2010) 143–148

Contents lists available at ScienceDirect

Journal of Electroanalytical Chemistry

journal homepage: www.elsevier.com/locate/jelechem

Characterization of growth of anodic antimony oxide films by ellipsometry and XPS

Omar E. Linarez Pérez [a], Miguel D. Sánchez [b], Manuel López Teijelo [a,*]

[a] INFIQC – Departamento de Fisicoquímica, Facultad de Ciencias Químicas, Universidad Nacional de Córdoba, Haya de la Torre y Medina Allende, 5000 Córdoba, Argentina
[b] Departamento de Física, Universidad Nacional del Sur and Planta Piloto de Ingeniería Química (UNS-CONICET), Camino La Carrindanga km. 7, 8000 Bahía Blanca, Argentina

ARTICLE INFO

Article history:
Received 5 November 2009
Received in revised form 4 February 2010
Accepted 29 April 2010
Available online 15 May 2010

Keywords:
Antimony oxide
Oxide growth
Ellipsometry
XPS

ABSTRACT

The processes occurring consecutively during anodic oxidation of antimony in buffered phosphate solutions are followed by *in situ* ellipsometry. In the first stages of anodization, soluble species formation followed by formation of a highly hydrated film takes place. At higher potentials, the growth of a single layer of Sb_2O_3 anodic film occurs. Oxygen evolution occurring simultaneously with oxide growth is also detected. Surface chemical analysis by XPS allowed obtaining the chemical state and composition of the anodic antimony oxide films. The procedure followed in order to carry out the spectra deconvolution due to overlapping of O1s and Sb3d photoemission lines is discussed. The binding energy values obtained for O1s and Sb3d signals as well as the O/Sb atomic ratio indicates that the anodic film formed at low or high potentials is composed by Sb(III) species only. Hydration as well as phosphate ions incorporation into the film is also demonstrated.

1. Introduction

Oxide films are widely applied in electrochemistry and passive films as well as their stability play an important role in present research [1]. Extensive studies on the properties and structure of the oxide films in relation to corrosion protection have also been performed. Electronically conducting oxide films have been used for applications in batteries or in electrocatalysis. On the other hand, passive oxide layers like those of the so-called "valve metals" (Al, Ta, Ti, etc.) are of the barrier type and show low ionic and electronic conductivity at low or medium field strengths ($\ll$1 MV cm^{-1}), which gives origin to growth of thick anodic oxide films by a "high-field" conduction behaviour [1]. Oxide films on ideal "valve metals" as Ta or Hf, usually grow by a field-assisted migration of ions though the film and other phenomena as oxide film dissolution or electron transfer contributions (e.g. oxygen evolution or other redox couples in solution) can be neglected. Other metals as W, Sb or even Al under certain conditions, present a more complex solution chemistry as well as electrochemical behaviour.

Antimony has been widely used as a constituent of alloys for lead–acid batteries, although antimony oxide (Sb_2O_3) has also found other applications as electrocatalyst, photoconductor, for thin film capacitors and in preparing electro chromic devices. The electrochemical behaviour of pure antimony has been mainly studied in sulphuric acid solutions [2–8], although some studies in other media as phosphoric acid or phosphate solutions [9–11] are found. In concentrated sulphuric solutions, Laihonen et al. [3] have established that Sb dissolves via the formation of trivalent antimony species (SbO^+) and even though the electrode potential is by far more positive than the equilibrium potential of the Sb(V)/Sb(III) couple, no pentavalent Sb species are formed. Based on electrochemical and scanning electron microscopy (SEM) measurements, Pavlov et al. [4,5] have determined that in sulphuric acid solutions the passive layers formed at low potentials values consist of amorphous and/or very thin antimony oxide or hydroxide. In addition, a simplified scheme for reactions assuming that the layer is built of amorphous SbOOH forming a gel-like film containing water that dissolves as SbO^+ species has also been proposed. Nevertheless, it has not been possible to ascribe the different oxidation and reduction peaks in the voltammograms and the presence of Sb_2O_3, Sb_2O_4 and Sb_2O_5 have been suggested in the literature. Electrochemical impedance spectroscopy was also employed in order to characterize the transport processes in the anodic films formed in sulphuric acid solutions [7,8]. More recently, the kinetics of growth, morphology and stability of antimony oxide films in buffered phosphate electrolytes by electrochemical methods, ellipsometry and atomic force microscopy, has been reported [11].

In order to determine the composition of the anodic layer formed during long-term polarization of antimony in concentrated sulphuric acid solutions, Laitinen et al. [6] have employed SEM, X-ray diffraction (XRD) and X-ray photoelectron spectroscopy (XPS) analysis. SEM results indicate that for films formed after 0.25–3 h of anodization, an amorphous layer consisting of antimony oxide and/or hydroxide is detected. At longer oxidation times (48 h) aggregates or crystals, which were identified by XRD as $Sb_4O_4(OH)_2SO_4$ and that correspond to a basic antimony

* Corresponding author. Tel.: +54 351 4334169; fax: +54 351 4334188.
E-mail address: mlopez@fcq.unc.edu.ar (M. López Teijelo).

1572-6657/$ - see front matter © 2010 Elsevier B.V. All rights reserved.
doi:10.1016/j.jelechem.2010.04.023

sulphate, are formed as an uppermost layer. The XPS analysis of composition and depth profile of the layers indicate that in sulphuric acid solutions anodic films consist of an outer part in which oxidized antimony, oxygen and sulphur are detected and an inner part which contain oxidized antimony and oxygen. Due to charging effects of the sample, the oxidation state of antimony in the oxide layer could not be determined. No other systematic investigation regarding the phase composition of the anodic layers formed on pure Sb during anodic polarization, in particular at high potentials, is found in the literature. Furthermore, XPS studies for chemical identification of species in antimony oxides prepared thermally [12,13], anodized InSb alloys [14–16], nanoparticles of Sb and Sb_2O_3 co-deposited galvanostatically [17] or by vapour condensation [18], have also been reported. For thermal oxides [13], the $3d_{3/2}$ binding energy values for Sb(III), Sb(IV) and Sb(V) oxides have been reported, but the Sb3d multiplet used for curve resolution was the $3d_{3/2}$ because the $3d_{5/2}$ overlaps the O1s peak. The same type of analysis has been made in order to identify the structure and composition of Sb_2O_3 nanoparticles [19]. From the information obtained, the authors conclude that deposited nanoparticles are composed by Sb_2O_3 and metallic Sb. Additionally, in the analysis for nanoparticles synthesized from antimony by vapour condensation, the contribution of the O1s signal in the 530 eV energy range has not been taken into account [18]. Chemical state identification by XPS of species during anodization of InSb alloys has also been reported [14–16]. For thin anodic oxide films formed on n-InSb (1 0 0) in aqueous solutions [15], based on the Sb4d doublet due to the overlapping of O1s and $Sb3d_{5/2}$ peaks, the results indicated In_2O_3 as the main oxide component, the presence of Sb_2O_3 and the total absence of Sb_2O_5. Similar conclusions have been reached in Ref. [16] but the species assignment is not correct. A different analysis was made in Ref. [14] for the structural characterization of oxide layers formed on the InSb surface. Due to the $Sb3d_{5/2}$ and O1s signals overlapping, the $Sb3d_{5/2}$ peak was deconvoluted by fixing the O1s peak position at 530.7 eV, which allowed concluding that anodic oxides were composed by $In_2O_3 + Sb_2O_3$. In addition, crystalline Sb_2O_3 thin films prepared by pulsed laser deposition and modified Pt surfaces by antimony underpotential deposition (upd) have been studied, although a thorough analysis of the XPS results has not been performed [20,21].

This work reports on the characterization by means of *in situ* ellipsometry of the different processes that take place sequentially during the anodic growth of antimony oxide films on pure antimony in buffered phosphate electrolytes in a wide potential range. Additionally, identification of species formed in the layers is made by XPS analysis.

2. Experimental

The working electrodes consisted of polycrystalline antimony rods (Goodfellow, 99.999% purity) of 6 mm diameter mounted in Teflon holders. A platinum sheet of 5 cm^2 was used as counter electrode. Potentials were measured versus the saturated calomel reference electrode (SCE). The surface of the antimony electrodes was pre-treated first with emery paper abrasion followed by mechanical polishing with 9, 3 and 1 μm diamond paste on a Nylon cloth and finishing with 0.05 μm Al_2O_3 on Microcloth (Buehler). Measurements were performed at 25 °C in aqueous solutions prepared from AR chemicals and purified water (Milli Ro–Milli Q system). 0.1 or 0.002 M ($NaH_2PO_4 + Na_2HPO_4$; pH = 7) solutions were employed as electrolyte. All solution used were deaerated by bubbling nitrogen before the oxide growth.

Electrochemical measurements were carried out using a 173 EG&G PAR potentiostat/galvanostat coupled to a 175 EG&G PARC signal generator and a 7090A Hewlett Packard plotting recorder. The anodic growth of the antimony oxide films was performed by anodic polarization of the mechanically polished antimony surfaces either applying linear potential sweeps or galvanostatically.

To characterize the optical behaviour during the growth of the anodic antimony oxide films, *in situ* ellipsometric measurements were performed during the electrochemical experiments. Optical measurements were carried out at a wavelength of 546.1 nm using a Rudolph research rotating-analyzer automatic ellipsometer (vertical type, 2000 FT model). The experimental setup has been previously described [11]. The optical properties of an isotropic single layer are given by its complex refractive index, $\boldsymbol{n} = n - ki$, where n stands for the refractive index and k for the extinction coefficient [22,23].

XPS measurements were made in a PHI 548 spectrometer using the Al Kα radiation at 250 W and 20 mA. The resolution spectra were taken at 50 eV pass energy at a base pressure better than 5×10^{-10} Torr. The C1s binding energy from adventitious hydrocarbon was taken as a charge reference and fixed at 284.5 eV. The signal deconvolution was made using Shirley type background subtraction and sum of asymmetric Gaussian–Lorentzian functions. The obtained binding energies were determined with a precision of 0.5 eV. The atomic ratio estimations were done relating the peak areas after the background subtraction and corrected relative to the corresponding atomic sensitivity factors. The samples were prepared by potentiodynamic polarization of mechanically polished surfaces until final potentials, E_f, of 3 and 8 V, followed by a potential holding of 30 min. Then, they were washed and dried with nitrogen before introducing in the vacuum pre-chamber. Additionally, the sample obtained by polarization at 3 V was etched by sputtering with Ar^+ primary ions generated at 2 keV and 30 mA.

3. Results and discussion

3.1. Electrochemical and ellipsometric behaviour

Fig. 1 shows the potentiodynamic and ellipsometric responses obtained at 0.1 V s^{-1} for a mechanically polished antimony electrode by applying a linear potential sweep in the −0.2 V to 10 V potential range. The description of this voltammogram (Fig. 1a) has already been done [11] and is shown for the sake of comparison. According to literature, the anodic peaks at low potentials have been attributed to electroformation of different antimony species with soluble species formation up to finally yield the Sb_2O_3 oxide [4,5], while the steady-state current obtained in the 0.9 V–3.5 V potential range has been attributed to the anodic growth of a Sb_2O_3 film by an ionic conduction mechanism caused by a "high-field" that drives the ionic migration as in typical "valve" metals [11]. However, no clear explanation of the processes taking place at potentials higher than *ca.* 3.5 V has been given. In this potential region, a poorly reproducible anodic current increase is observed before reaching the massive oxygen evolution at potentials close to 10 V (Fig. 1a). An oxygen evolution contribution taking place well-before the massive oxygen evolution jointly with oxide growth as well as the formation of a Sb_2O_5 anodic film have been proposed [3,6]. Therefore, in order to clarify the nature of the processes taking place during anodic growth in a wide range of potentials as well as identify the species formed, ellipsometric and XPS measurements were performed.

In situ ellipsometry is a very sensitive tool for studying changes in the optical properties of an electrochemical interface, exhibiting a high sensitivity to changes in surface processes. In addition, it is specially suited for detecting different processes that take place sequentially, even though is not able of identify chemical species.

The optical Ψ and Δ response obtained during potentiodynamic growth at 0.1 V s^{-1} is shown in Fig. 1b. The first stages of the

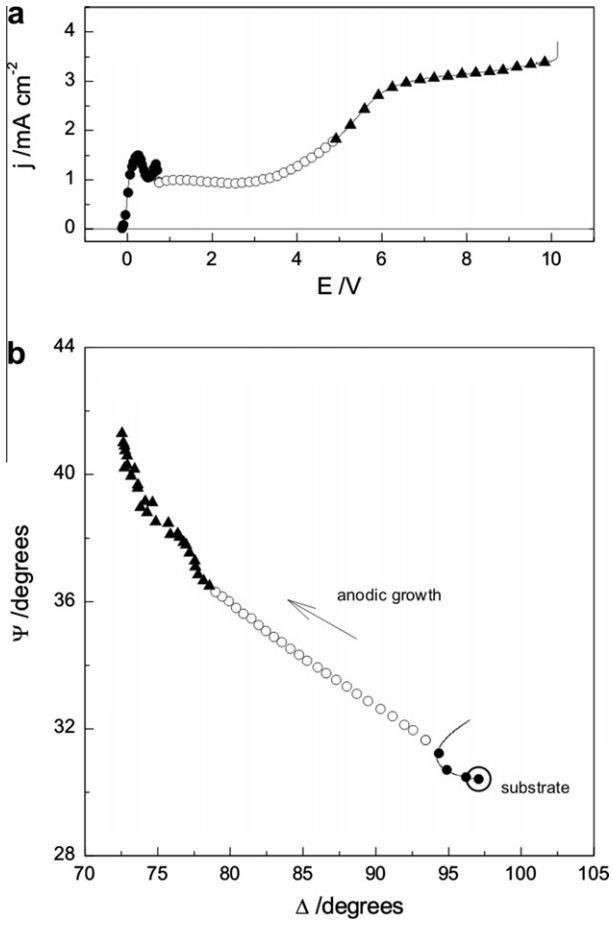

Fig. 1. Potentiodynamic *j*/*E* (a) and $\Psi-\Delta$ (b) responses during the potentiodynamic growth of a Sb_2O_3 film on a mechanically polished antimony surface. 0.1 M [NaH_2PO_4 + Na_2HPO_4] (pH = 7); υ = 0.1 V s^{-1}. (○) Mechanically polished substrate; (—) simulation for growth of an isotropic film with $\boldsymbol{n_f}$ = 1.35–0.008*i*.

growth (−0.2 V to 0.9 V range) define a small loop in the $\Psi-\Delta$ plane, which corresponds to the growth of a thin film having a low refractive index (n_f) value. A rough estimation of the optical constants in this potential range gives $n_f = 1.35 - 0.008i$ for the complex refractive index (see simulation in Fig. 1b). The low value of refractive index (n_f = 1.35) corresponds to the anodic growth of a highly hydrated oxide/hydroxide film in the low potentials region [23]. This is in agreement with literature results where the formation of an amorphous and gel-like anodic SbOOH film has been proposed [5,6]. At potentials higher than *ca.* 1.0 V, the optical response (open symbols) shows the typical changes associated with the growth of an oxide film [24–27], but at potentials exceeding around 4.5 V (full triangles) the $\Psi-\Delta$ response shows an increasing scattering and the formation of oxygen bubbles on the surface is seen. The evaluation of optical properties as well as thickness of the anodic oxide film at high potentials has been made by employing galvanostatic methods, as reported recently [11].

Furthermore, antimony oxide films were also grown under galvanostatic conditions. The potential/time dependence obtained during the galvanostatic growth (j = 2.14 mA cm^{-2}) of an antimony oxide film up to 14 V (Fig. 2) shows a potential increase (up to *ca.* 2 V) and, after a break, potential rises linearly with time, as expected for oxide growth on "valve" metals [28]. Fig. 3 shows the changes of Ψ and Δ with time in the first 30 s of galvanostatic anodization. In the first 10 s, which correspond to a potential value of *ca.* 2 V in the *E*/*t* curve, Ψ and Δ present a very small change with time in relation to the initial values for the mechanically

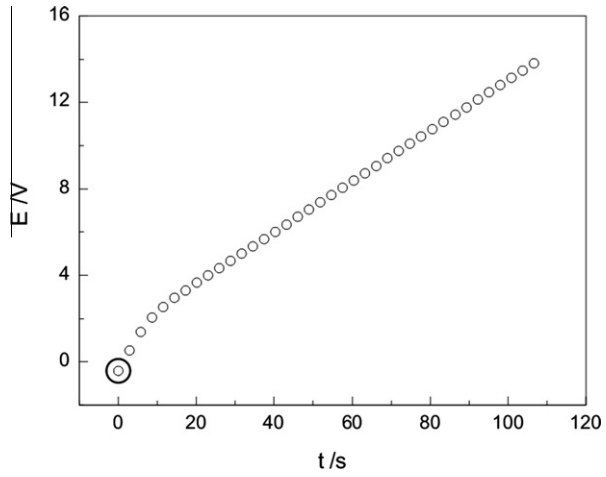

Fig. 2. Galvanostatic *E*/*t* response during the galvanostatic growth of a Sb_2O_3 film on a mechanically polished antimony surface. 0.002 M [NaH_2PO_4 + Na_2HPO_4] (pH = 7); j = 2.14 mA cm^{-2}. (○) Mechanically polished surface.

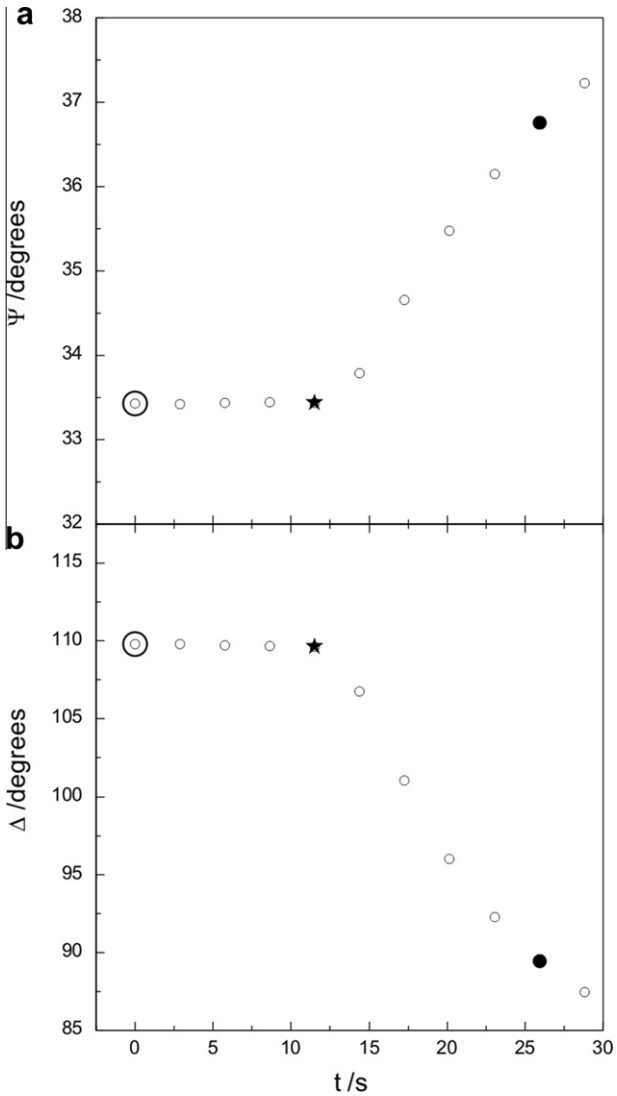

Fig. 3. Dependence of Ψ (a) and Δ (b) with time during the galvanostatic growth of a Sb_2O_3 film on a mechanically polished antimony surface. 0.002 M [NaH_2PO_4 + Na_2HPO_4] (pH = 7); j = 2.14 mA cm^{-2}. (○) Mechanically polished surface; (★) 2 V; (●) 4 V.

polished antimony surface. This indicates that under galvanostatic conditions and during the time necessary for reaching the potential region where the break in the E/t curve is obtained, the anodic process would correspond mainly to the formation of soluble species followed by the formation of a very thin and hydrated film. After that, the typical changes in the Ψ and Δ values corresponding to a thick film growth are obtained. These results are interpreted as the formation of soluble species in the first stages and, when concentration of antimony species close to the electrode surface exceeds a certain value, formation of a surface oxide film and further growth take place.

3.2. XPS characterization

X-ray photoelectron spectroscopy (XPS), a surface chemical analysis technique, was employed for obtaining the chemical state and composition of the anodic antimony oxide films. In order to identify the different antimony oxides that can be formed in the different potential regions, XPS spectra for films grown up to E_f = 3 V and 8 V were obtained (Fig. 4). In the 525–545 eV energy range, spectra consist of two well-defined peaks that show a complicated feature due to the overlapping of O1s and $Sb3d_{5/2}$ photoemission lines around 531 eV [12]. Because of this, in most of work found in literature [13–21] the deconvolution of $Sb3d_{5/2}$ and O1s signals has no been performed and, in some cases, the species assignment was based only in the energy of the overall maxima in the spectra. Partial deconvolution of the experimental data [13,14,19], analysis of a less intense Sb photoemission line [15] or erroneous species assignment [16,18] have been reported. Furthermore, crystalline Sb_2O_3 thin films prepared by pulsed laser deposition and modified Pt surfaces via upd deposition have been studied, although a thorough analysis of the XPS results has not been performed [20,21].

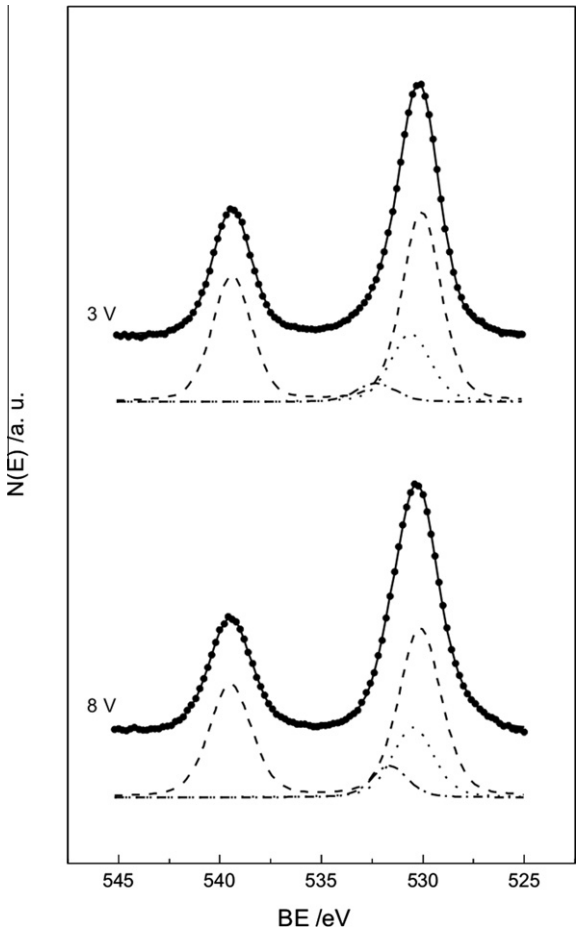

Fig. 4. Sb3d and O1s XPS peaks obtained for anodic films grown up to E_f = 3 V and 8 V in 0.1 M $NaH_2PO_4 + Na_2HPO_4$ (pH = 7). (●●●) Experimental and (—) fitted spectra; (- - - -) Sb3d, (···) O1s(I) and (–·–·–) O1s(II) contributions. Spectra have been shifted for clarity.

Therefore, in the present work the spectra deconvolution was carried out taking into account the spin–orbit coupling fixing the $Sb3d_{3/2}/Sb3d_{5/2}$ area ratio to 2:3 and the doublet splitting energy in 9.3 eV [12] in order to quantify the individual contributions of the Sb3d and O1s lines [29]. Additionally, two O1s signals, denoted by O1s(I) and O1s(II), were necessary in the fitting procedure to obtain the best correlation. Fig. 4 also shows the different contributions obtained from the fitting procedure described above. The $Sb3d_{5/2}$ and $Sb3d_{3/2}$ peaks appear at 530.1 or 530.3 eV and 539.4 or 539.6 eV, for anodic antimony oxide films grown up to 3 V and 8 V, respectively, which matches well with the literature values for oxidized Sb(III) species [12,14,15,17]. No other antimony species contributions corresponding to Sb(IV) or Sb(V), which appear at slightly higher binding energies [13], are seen. On the other hand, the O1s(I) peak is obtained at 530.6 or 530.7 eV whereas the O1s(II) contribution appears at 532.3 or 531.8 eV for oxide films grown at 3 V and 8 V, respectively. The energy of the O1s(I) peak is assigned to the oxygen directly bounded to antimony in the oxide lattice, O–Sb [12,30], while the O1s(II) peak may arise due to the presence of water and hydroxyl species or other oxygen-containing species incorporated in the film [12,31,32]. O1s signals at around the same energies have been reported previously and attributed to oxygen in metal–oxygen bond and in OH^- ions and bound water for thermal antimony oxide [12,30] and anodic oxides formed in Cr–Nb alloys [31]. Furthermore, the O1s(I)/Sb3d atomic ratio for oxide layers formed at 3 or 8 V calculated from peak areas and taking into account the corresponding atomic sensitivity factors [12], is estimated in around 1.4, corroborating the Sb_2O_3 stoichiometry for both anodic oxide films. This result for films formed at low or high potentials is also in agreement with the absence of antimony oxides with oxidation state higher than +3.

Additional evidence of the chemical state of the oxide layers was obtained from depth profiles made by XPS analysis after a sputtering period with argon (Fig. 5). During the sputtering process the oxide film thickness decreases locally and the underneath antimony metallic surface begins to be exposed, resulting in an additional Sb3d signal corresponding to metallic antimony at lower binding energies. Fig. 5 also shows the spectrum deconvolution employing the Sb3d doublets for oxidized and metallic antimony as well as the O1s contribution. The photoemission lines for metallic antimony are shifted 2.5 eV to lower binding energies in agreement with values reported in the literature [12,17], being an indication that the anodic film is composed only by Sb(III) species.

The growth of anodic oxide films on different metals is usually accompanied by incorporation of species from the electrolyte into the oxide [15,28,31,33–37]. Besides the chemical state and composition of the antimony oxide films, the incorporation of phosphate ions was analyzed. Fig. 6 shows the P2p XPS spectra for the samples described previously as well as the fitted curves fixing the $P2p_{1/2}/P2p_{3/2}$ area ratio to 1:2 and the doublet splitting energy in 0.8 eV [12]. The $P2p_{3/2}$ signals appear at 133.1–133.2 eV for both, 3 V and 8 V samples, which agrees with literature values [12,15,28,32,35,37]. This evidence indicates that incorporation of phosphate ions into Sb_2O_3 films takes place. The calculated P/Sb atomic ration in the outer part for oxide layers formed at 3 or 8 V, are around 0.1 and 0.35, respectively. Incorporation of water and/or phosphate species is also in agreement with the lower values of the refractive indices reported for anodic antimony oxides as compared with known crystalline oxides [11].

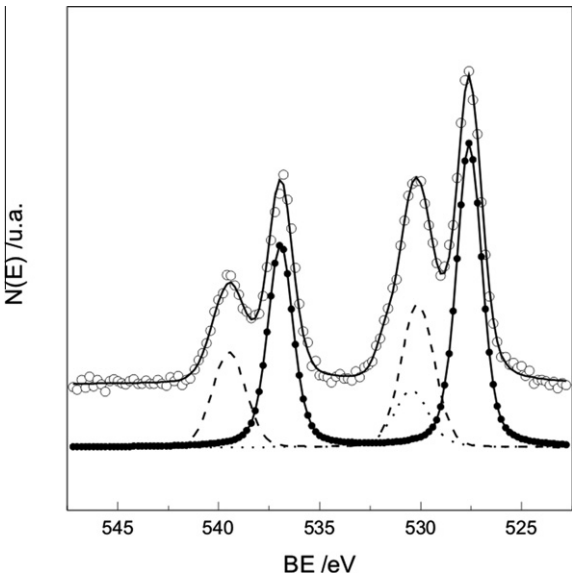

Fig. 5. Sb3d and O1s XPS peaks obtained for an anodic film grown up to E_f = 3 V in 0.1 M NaH_2PO_4 + Na_2HPO_4 (pH = 7), after argon sputtering. (○○○) Experimental and (—) fitted spectra; (- - - -) Sb(III) and (●●●) Sb(0) contributions; (···) O1s. Spectra have been shifted for clarity.

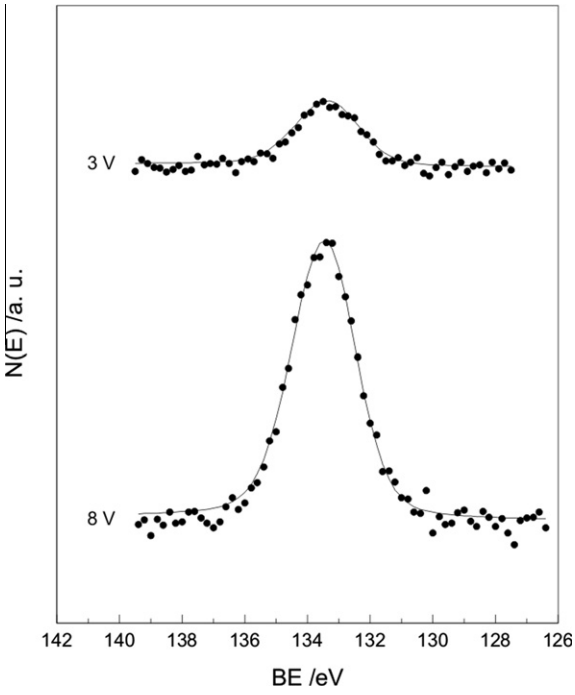

Fig. 6. P2p XPS spectra obtained for anodic films grown up to E_f = 3 V and 8 V in 0.1 M NaH_2PO_4 + Na_2HPO_4 (pH = 7). (●●●) Experimental and (—) fitted spectra.

In summary, XPS results indicate that anodic films are composed of Sb_2O_3 at low and high potentials. This also correlates well with ellipsometric results previously reported [11], which indicate that antimony oxide films grown in the 2–14 V potential range, have optical properties that do not change during growth and, consequently, are of the same nature.

4. Conclusions

The electrochemical and ellipsometric results for the anodization of antimony in buffered phosphate electrolytes indicate that at low potentials the anodic behaviour can be interpreted in terms of the formation of soluble species in the first stages of anodization followed by the formation of an amorphous and highly hydrated film. At higher potentials, a single layer of Sb_2O_3 grows in a wide potential range. In addition, a contribution of oxygen evolution is also detected at potentials higher than *ca.* 4.5 V.

The chemical state and composition of the anodic antimony oxide at different potentials were obtained from XPS measurements. The spectra deconvolution corresponding to Sb3d and O1s photoemission lines was performed fixing the $Sb3d_{3/2}/Sb3d_{5/2}$ area ratio in 2:3 and the Sb3d doublet splitting energy in 9.3 eV. Two O1s contributions were obtained from the fitting procedure, which are attributed to oxygen bounded to antimony in the oxide latticed and to water or other oxygen-containing species incorporated in the film. The binding energy values obtained for $Sb3d_{3/2}$ and $Sb3d_{5/2}$ emission lines are in agreement with those corresponding to oxidized Sb(III) species and no contributions of other antimony species are detected. Binding energies of Sb3d photoemission lines corresponding to metallic antimony in argon sputtered samples are shifted to lower energies in values that are also compatible with formation of Sb(III) species. Furthermore, the O/Sb atomic ratio also corroborates the Sb_2O_3 formation at both low and high potentials. Incorporation of water as well as phosphate species from the electrolyte is also demonstrated from XPS experiments.

Acknowledgements

Financial support from the Consejo Nacional de Investigaciones Científicas y Técnicas of Argentina (CONICET), the Agencia Nacional de Promoción Científica y Tecnológica (ANPCYT), and the Secretaría de Ciencia y Tecnología (SECYT-UNC) is gratefully acknowledged. OELP thanks CONICET for the fellowships granted.

References

[1] J.W. Schultze, M.M. Lohrengel, Electrochim. Acta 45 (2000) 2499.
[2] M. Metikoš-Huković, B. Lovreček, Electrochim. Acta 25 (1980) 717.
[3] S. Laihonen, T. Laitinen, G. Sundholm, A. Yli-Pentti, Electrochim. Acta 35 (1990) 229.
[4] D. Pavlov, M. Bojinov, T. Laitinen, G. Sundholm, Electrochim. Acta 36 (1991) 2081.
[5] D. Pavlov, M. Bojinov, T. Laitinen, G. Sundholm, Electrochim. Acta 36 (1991) 2087.
[6] T. Laitinen, H. Revitzer, G. Sundholm, J.K. Vilhunen, D. Pavlov, M. Bojinov, Electrochim. Acta 36 (1991) 2093.
[7] M. Bojinov, I. Kanazirsky, A. Girginov, Electrochim. Acta 41 (1996) 2695.
[8] M. Metikoš-Huković, R. Babić, S. Brinić, J. Power Sources 157 (2006) 563.
[9] M.M. Hefny, W.A. Badawy, A.S. Mogoda, M.S. El-Basiouny, Electrochim. Acta 30 (1985) 1017.
[10] M. Bojinov, I. Kanazirski, A. Girginov, Electrochim. Acta 40 (1995) 873.
[11] O.E. Linarez Pérez, M.A. Pérez, M. López Teijelo, J. Electroanal. Chem. 632 (2009) 64.
[12] J.F. Moulder, W.F. Stickle, P.E. Sobol, K.D. Bomben, J. Chastain (Eds.), Handbook of X-ray Photoelectron Spectroscopy, Perkin–Elmer Corp., USA, 1992.
[13] R. Izquierdo, E. Sacher, A. Yelon, Appl. Surf. Sci. 40 (1989) 175.
[14] A. Rastogi, K.V. Reddy, Thin Solid Films 270 (1995) 616.
[15] L. Santinacci, G.I. Sproule, S. Moisa, D. Landheer, X. Wu, A. Banu, T. Djenizian, P. Schmuki, M.J. Graham, Corros. Sci. 46 (2004) 2067.
[16] A. Suleiman, T. Hashimoto, P. Skeldon, G.E. Thomson, F. Echeverria, M.J. Graham, G.I. Sproule, S. Moisa, H. Habazaki, P. Bailey, T.C.Q. Noakes, Corros. Sci. 50 (2008) 1353.
[17] H. Bryngelsson, J. Eskhult, L. Nyholm, M. Herranen, O. Alm, K. Edström, Chem. Mater. 19 (2007) 1170.
[18] D.W. Zeng, C.S. Xie, B.L. Zhu, W.L. Song, Mater. Lett. 58 (2004) 312.
[19] D.W. Zeng, B.L. Zhu, C.S. Xie, W.L. Song, A.H. Wang, Mater. Sci. Eng. A 366 (2004) 332.
[20] M.Z. Xue, Z.W. Fu, Electrochem. Commun. 8 (2006) 1250.
[21] J.K. Lee, H. Jeon, S. Uhm, J. Lee, Electrochim. Acta 53 (2008) 6089.
[22] R.M.A. Azzam, N.M. Bashara, Ellipsometry and Polarized Light, North Holland, Amsterdam, 1977.
[23] S. Gottesfeld, in: A.J. Bard (Ed.), Electroanalytical Chemistry, vol. 15, Marcel Dekker, New York, 1989, p. 143.
[24] M.A. Pérez, M. López Teijelo, Thin Solid Films 449 (2004) 138.
[25] M.A. Pérez, M. López Teijelo, J. Phys. Chem. B 109 (2005) 19369.
[26] M.A. Pérez, M. López Teijelo, J. Electroanal. Chem. 583 (2005) 212.

[27] M.A. Pérez, O.E. Linarez Pérez, M. López Teijelo, J. Electroanal. Chem. 596 (2006) 149.
[28] C.E.B. Marino, P.A.P. Nascente, S.R. Biaggio, R.C. Rocha-Filho, N. Bocchi, Thin Solid Films 468 (2004) 109.
[29] D. Briggs, J.T. Grant. (Eds.), Surface Analysis by Auger and X-ray Photoelectron Spectroscopy, 2003 IM Publication and Surface Spectra Limited.
[30] C.D. Wagner, D.A. Zatko, R.H. Raymond, Anal. Chem. 52 (1980) 1445.
[31] X.Y. Li, E. Akiyama, H. Habazaki, A. Kawashima, K. Asami, K. Hashimoto, Corros. Sci. 40 (1998) 821.
[32] M.B.J.G. Freitas, C. Eiras, L.O.S. Bulhões, Corros. Sci. 46 (2004) 1051.
[33] J.S. Llewelyn Leach, B.R. Pearson, Electrochim. Acta 29 (1984) 1263.
[34] K. Shimizu, H. Habazaki, P. Skeldon, G.E. Thompson, G.C. Wood, Electrochim. Acta 45 (2000) 1805.
[35] K. Shimizu, G.M. Brown, H. Habazaki, K. Kobayashi, P. Skeldon, G.E. Thompson, G.C. Wood, Corros. Sci. 40 (1998) 963.
[36] N. Khalil, J.S.L. Leach, Electrochim. Acta 40 (1994) 1769.
[37] K. Shimizu, G.M. Brown, H. Habazaki, K. Kobayashi, P. Skeldon, G.E. Thompson, G.C. Wood, Corros. Sci. 41 (1999) 1971.